

Many-Body Approaches to Quantum Dots

Patrick Merlot

Department of Computational Physics

November 4, 2009

Table of contents

- 1 Quantum Dots
- 2 Model, Methods and Implementation
- 3 Results and Discussions

Table of contents

- 1 Quantum Dots
 - What is a quantum dot?
 - Physics of QDs
 - Applications of QDs
- 2 Model, Methods and Implementation
- 3 Results and Discussions

What is a quantum dot?

Definition

- Semiconductor whose charge-carriers are confined in space.
- \neq types/shapes/fabrication
 $\Rightarrow \neq$ QDs

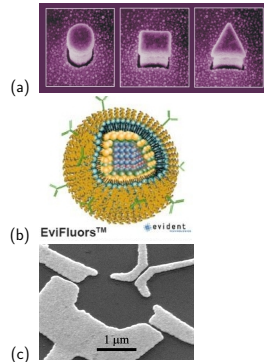


Figure 1: Possible types/shapes of QDs.

- (a) Various shapes of QDs pillars $\sim 0.5 \mu\text{m}$,
(b) Colloidal QD (InGaP+ZnS+lipid) $\sim 10 \text{nm}$,
(c) QD defined by 5 metallic gates on GaAs where 2-DEG is trapped.

Physics of QDs

Quantum dot properties

- Semiconductor band gap increased by size quantization

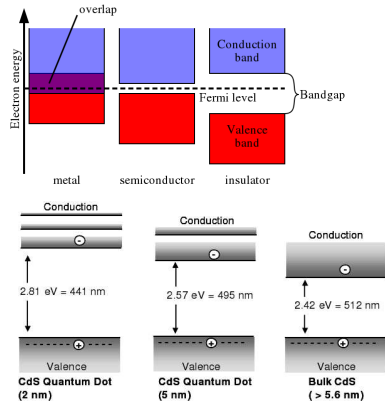


Figure 2: Electronic band structure of semiconductor and quantum dots (Courtesy of J.Winter[4]).

Physics of QDs

Quantum dot properties

- Semiconductor band gap increased by size quantization
- Tunable optical/electrical properties
- Perfect system for computational studies

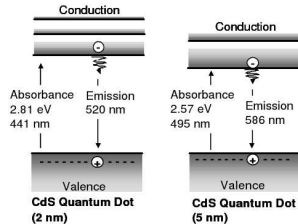


Figure 3: Fluorescent emission (Courtesy of J.Winter[4]).

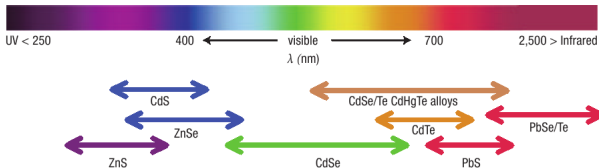


Figure 4: Emission spectra of various quantum dots.

Applications of QDs

Possible applications

- Biological nano-sensors
- Qubits for QCA
- LEDs
- Solar cells

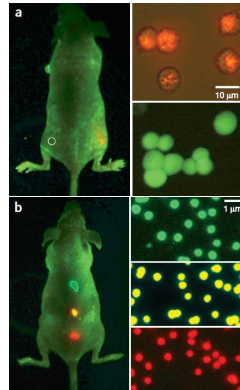


Figure 5: QDs imaging in live animals compared to classical organic dyes. (Courtesy of X. Gao)

Table of contents

1 Quantum Dots

2 Model, Methods and Implementation

- Model of a quantum dot
- The method of Variational calculus
- The Hartree-Fock method
- The many-body perturbation theory
- Implementation

3 Results and Discussions

Model of a quantum dot

Simple model of a quantum dot

- **Atomic scale problem** \Rightarrow **Quantum mechanics** for an accurate description of the system.
 \Rightarrow at rest, solve the time-independent Schrödinger equation $\hat{H}|\Psi\rangle = E|\Psi\rangle$.
- Not modelling all nuclei/electrons \Rightarrow just model the few quasiparticles confined by the semiconductor.

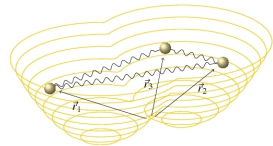
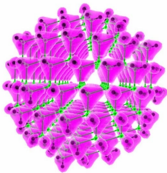


Figure 6: Illustration of a quantum dot model (Courtesy of S.Kvaal[5]).

Model of a N -particle system

The Schrödinger equation

- The Schrödinger equation of a N -particle system

$$\hat{H}(\mathbf{r}_1, \mathbf{r}_2, \dots, \mathbf{r}_N) |\Psi_\kappa(\mathbf{r}_1, \mathbf{r}_2, \dots, \mathbf{r}_N)\rangle = E_\kappa |\Psi_\kappa(\mathbf{r}_1, \mathbf{r}_2, \dots, \mathbf{r}_N)\rangle \quad (1)$$

where \mathbf{r}_i represents the (spatial/spin) coordinates of quasiparticle i ,
 κ stands for all quantum numbers needed to classify a given
 N -particle state,
 $|\Psi_\kappa\rangle$ and E_κ are the eigenstates and eigenenergies of the system.

How to define our Hamiltonian?

- $$\hat{H} = \sum_{i=1}^{N_e} \frac{\mathbf{p}_i^2}{2m^*} + \dots$$

Definitions of the interactions/potentials

Forces/Fields acting on the quasiparticles:

- Forces confining the particles \Rightarrow **Confining potential**
- Interactions between the particles \Rightarrow **Interaction potential**

The Hamiltonian of our two-electron quantum dot model

- Confining potential \Rightarrow **the harmonic oscillator (parabolic) potential**

$$\hat{H} = \sum_{i=1}^{N_e=2} \frac{\mathbf{p}_i^2}{2m^*} + \sum_{i=1}^{N_e=2} \frac{1}{2} m^* \omega_0^2 \|\mathbf{r}_i\|^2 + \frac{e^2}{4\pi\epsilon_0\epsilon_r} \frac{1}{\|\mathbf{r}_1 - \mathbf{r}_2\|}, \quad (2)$$

- Interaction potential \Rightarrow **the two-body Coulomb interaction**

Applying an external magnetic field

① $\mathbf{p}_i \longrightarrow \mathbf{p}_i + e\mathbf{A}$, where \mathbf{A} is the vector potential defined by $\mathbf{B} = \nabla \times \mathbf{A}$.

• in coordinate space $\mathbf{p}_i \rightarrow -i\hbar\nabla_i$,

• using a Coulomb gauge $\nabla \cdot \mathbf{A} = 0$ (by choosing $\mathbf{A}(\mathbf{r}_i) = \frac{\mathbf{B} \times \mathbf{r}_i}{2}$),

$$(\mathbf{p}_i + e\mathbf{A})^2 \rightarrow \left(-\frac{\hbar^2}{2m^*} \nabla_i^2 - i\hbar \frac{e}{m^*} \mathbf{A} \cdot \nabla_i + \frac{e^2}{2m^*} \mathbf{A}^2 \right). \quad (3)$$

In terms of \mathbf{B} , the linear and quadratic terms in \mathbf{A} have the form

$$\frac{-i\hbar e}{m^*} \mathbf{A} \cdot \nabla_i = \frac{e}{2m^*} \mathbf{B} \cdot \mathbf{L}, \text{ and } \frac{e^2}{2m^*} \mathbf{A}^2 = \frac{e^2}{8m^*} B^2 r_i^2. \text{ where } \mathbf{L} = -i\hbar(\mathbf{r}_i \times \nabla_i)$$

is the orbital angular momentum operator of the electron i .

② \mathbf{B} also acts on spin with the additional energy term: $\hat{H}_s = g_s^* \frac{\omega_c}{2} \hat{S}_z$, where \hat{S}

is the spin operator of the electron and g_s^* is its effective spin gyromagnetic ratio and $\omega_c = eB/m^*$ is known as the cyclotron frequency.

Final Hamiltonian

The final Hamiltonian reads:

$$\begin{aligned}
 \hat{H} = & \sum_{i=1}^{N_e} \left(\frac{-\hbar^2}{2m^*} \nabla_i^2 + \overbrace{\frac{1}{2} m^* \omega_0^2 \|\mathbf{r}_i\|^2}^{\text{Harmonic oscillator potential}} \right) + \overbrace{\frac{e^2}{4\pi\epsilon_0\epsilon_r} \sum_{i<j} \frac{1}{\|\mathbf{r}_i - \mathbf{r}_j\|}}^{\text{Coulomb interactions}} \\
 & + \underbrace{\sum_{i=1}^{N_e} \left(\frac{1}{2} m^* \left(\frac{\omega_c}{2} \right)^2 \|\mathbf{r}_i\|^2 + \frac{1}{2} \omega_c \hat{L}_z^{(i)} + \frac{1}{2} g_s^* \omega_c \hat{S}_z^{(i)} \right)}_{\text{single particle interactions with the magnetic field}}, \quad (4)
 \end{aligned}$$

Scaling the problem: dimensionless form of \hat{H}

New constant, the oscillator frequency $\omega = \sqrt{\omega_0 + \left(\frac{\omega_c}{2}\right)^2}$,

New units:

- the energy unit $\hbar\omega$,
- the length unit, the oscillator length defined by $l = \sqrt{\hbar/(m^*\omega)}$.

The dimensionless Hamiltonian is now

$$\hat{H} = \sum_{i=1}^{N_e} \left[-\frac{1}{2} \nabla_i^2 + \frac{1}{2} r_i^2 \right] + \lambda \sum_{i < j} \frac{1}{r_{ij}} + \sum_{i=1}^{N_e} \left(\frac{1}{2} \frac{\omega_c}{\hbar\omega} m_l^{(i)} + \frac{1}{2} g_s^* \frac{\omega_c}{\hbar\omega} m_s^{(i)} \right). \quad (5)$$

where the new dimensionless parameter $\lambda = l/a_0^*$ describes the strength of the electron-electron interaction (a_0^* being the effective Bohr radius).

The Hamiltonian solved in this project

$$\lambda(B) = \frac{1}{a_0^*} \left(\frac{4\hbar^2}{4\omega_0^2 m^{*2} + e^2 B^2} \right)^{\frac{1}{4}}$$

Role of B?

- Squeezing the particles should increase the strength of the electron-electron interaction.
- λ only decreases as the magnetic field increases in this model.

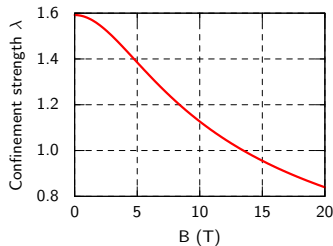


Figure 7: Dimensionless confinement strength λ as a function of the magnetic field strength in GaAs.

In the rest of the project, we will solve the following Hamiltonian:

$$\hat{H} = \sum_{i=1}^{N_e} \left[-\frac{1}{2} \nabla_i^2 + \frac{1}{2} r_i^2 \right] + \lambda \sum_{i < j} \frac{1}{r_{ij}}. \quad (6)$$

The method of variational calculus

Definition

Method to solve the Schrödinger eq. more efficiently than using numerical integration.

- Based on the method of Lagrange multipliers, where the functional to minimize (the energy functional) is an integral over the unknown wave function $|\Phi\rangle$

$$E[\Phi] = \frac{\langle \Phi | H | \Phi \rangle}{\langle \Phi | \Phi \rangle} = \frac{\int \Phi^* H \Phi d\tau}{\int \Phi^* \Phi d\tau}, \quad (7)$$

while subject to a normalization constraint $\langle \Phi | \Phi \rangle = 1$.

- The method introduces new variables for each of the constraints (the Lagrange multipliers ϵ) and defines the Lagrangian (Λ) with respect to $|\Phi\rangle$ as

$$\Lambda(\Phi, \epsilon) = E[\Phi] - \epsilon (\langle \Phi | \Phi \rangle - 1), \quad (8)$$

- Find stationary solutions by solving the set of equations by writing $\frac{\partial \Lambda}{\partial \Phi} = 0$.

The Hartree-Fock method

Definition

The HF method is a particular case of variational method in accordance with

- the independent particle approximation,
- the Pauli exclusion principle.

The approximated wave function

To fulfill these criteria, the wave-function must be antisymmetric with respect to an interchange of any two particles:

$$\Phi(\mathbf{r}_1, \mathbf{r}_2, \dots, \mathbf{r}_i, \dots, \mathbf{r}_j, \dots, \mathbf{r}_N) = -\Phi(\mathbf{r}_1, \mathbf{r}_2, \dots, \mathbf{r}_j, \dots, \mathbf{r}_i, \dots, \mathbf{r}_N). \quad (9)$$

The Hartree-Fock wave function

The **Slater determinant** is an antisymmetric product of the single particle orbitals:

$$\Phi(\mathbf{r}_1, \mathbf{r}_2, \dots, \mathbf{r}_N, \alpha, \beta, \dots, \sigma) = \frac{1}{\sqrt{N!}} \begin{vmatrix} \psi_\alpha(\mathbf{r}_1) & \psi_\alpha(\mathbf{r}_2) & \dots & \psi_\alpha(\mathbf{r}_N) \\ \psi_\beta(\mathbf{r}_1) & \psi_\beta(\mathbf{r}_2) & \dots & \psi_\beta(\mathbf{r}_N) \\ \vdots & \vdots & \ddots & \vdots \\ \psi_\sigma(\mathbf{r}_1) & \psi_\sigma(\mathbf{r}_2) & \dots & \psi_\sigma(\mathbf{r}_N) \end{vmatrix}, \quad (10)$$

It can be rewritten as

$$\Phi_T(\mathbf{r}_1, \mathbf{r}_2, \dots, \mathbf{r}_N, \alpha, \beta, \dots, \sigma) = \frac{1}{\sqrt{N!}} \sum_p (-)^p \Psi_\alpha(\mathbf{r}_1) \Psi_\beta(\mathbf{r}_2) \dots \Psi_\sigma(\mathbf{r}_N) \quad (11)$$

$$= \sqrt{N!} \mathcal{A}(\Psi_\alpha(\mathbf{r}_1) \Psi_\beta(\mathbf{r}_2) \dots \Psi_\sigma(\mathbf{r}_N)), \quad (12)$$

by introducing the **antisymmetrization operator** $\mathcal{A} = \frac{1}{N!} \sum_p (-)^p \hat{P}$.

Matrix elements calculations

Definition

We write the Hamiltonian for N electrons as $\hat{H} = \hat{H}_0 + \hat{H}_1 = \sum_{i=1}^N \hat{h}_i + \sum_{i<j}^N v(\mathbf{r}_i, \mathbf{r}_j)$,

where $r_{ij} = \|\vec{r}_i - \vec{r}_j\|$, \hat{h}_i and $v(\mathbf{r}_i, \mathbf{r}_j)$ are respectively the one-body and the two-body Hamiltonian.

Using properties of \mathcal{A} and commutation rule with \hat{H}_0 and \hat{H}_1 , one can write:

$$\int \Phi_T^* \hat{H}_0 \Phi_T d\tau = \sum_{\mu=1}^N \int \Psi_{\mu}^*(\mathbf{r}) \hat{h} \Psi_{\mu}(\mathbf{r}) d\mathbf{r} = \sum_{\mu=1}^N \langle \mu | h | \mu \rangle. \quad (13)$$

$$\int \Phi_T^* \hat{H}_1 \Phi_T d\tau = \frac{1}{2} \sum_{\mu=1}^N \sum_{\nu=1}^N \langle \mu\nu | V | \mu\nu \rangle_{AS}. \quad (14)$$

where we define the antisymmetrized matrix element as

$\langle \mu\nu | V | \mu\nu \rangle_{AS} = \langle \mu\nu | V | \mu\nu \rangle - \langle \mu\nu | V | \nu\mu \rangle$, with the following shorthands

$$\langle \mu\nu | V | \mu\nu \rangle = \int \Psi_{\mu}^*(\mathbf{r}_i) \Psi_{\nu}^*(\mathbf{r}_j) V(r_{ij}) \Psi_{\mu}(\mathbf{r}_i) \Psi_{\nu}(\mathbf{r}_j) d\mathbf{r}_i d\mathbf{r}_j.$$

The Hartree-Fock energy in the harmonic oscillator basis

The energy functional

The energy functional is our starting point for the Hartree-Fock calculations.

$$E[\Phi_T] = \langle \Phi_T | \hat{H}_0 | \Phi_T \rangle + \langle \Phi_T | \hat{H}_1 | \Phi_T \rangle \quad (15)$$

$$= \sum_{\mu=1}^N \langle \mu | h | \mu \rangle + \frac{1}{2} \sum_{\mu=1}^N \sum_{\nu=1}^N \langle \mu \nu | V | \mu \nu \rangle_{AS}. \quad (16)$$

We expand each single-particle eigenvector Ψ_i in terms of a convenient complete set of single-particle states $|\alpha\rangle$ (the harmonic oscillator eigenstates in our case),

$$\Psi_i = |i\rangle = \sum_{\alpha} c_i^{\alpha} |\alpha\rangle. \quad (17)$$

The energy functional now reads

$$E[\Phi] = \sum_{i=1}^N \sum_{\alpha\gamma} C_i^{\alpha*} C_i^{\gamma} \langle \alpha | h | \gamma \rangle + \frac{1}{2} \sum_{i,j=1}^N \sum_{\alpha\beta\gamma\delta} C_i^{\alpha*} C_j^{\beta*} C_i^{\gamma} C_j^{\delta} \langle \alpha\beta | V | \gamma\delta \rangle_{AS}. \quad (18)$$

The Hartree-Fock equations (1)

Remember the method of the Lagrange multipliers

- 1 Define a functional $E[\Phi_T]$,
- 2 Identify the constraints: $\langle \Psi_i | \Psi_j \rangle = \delta_{ij}$ which implies $\langle \Phi_T | \Phi_T \rangle = 1$,
with $\langle \Psi_i | \Psi_j \rangle = \sum_{\alpha\beta} C_i^{\alpha*} C_j^\beta \underbrace{\langle \alpha | \beta \rangle}_{\delta_{\alpha\beta}} = \sum_{\alpha} C_i^{\alpha*} C_j^\alpha$

- 3 Define the Lagrangian Λ

$$\Lambda(C_1^\alpha, C_2^\alpha, \dots, C_N^\alpha, \epsilon_1, \epsilon_2, \dots, \epsilon_N) = E[\Phi_T] - \sum_{i=1}^N \epsilon_i \left(\sum_{\alpha} C_i^{\alpha*} C_i^\alpha - \delta_{ii} \right). \quad (19)$$

where ϵ_i are the Lagrange multipliers for each of the normalization constraints.

- 4 Get the system of equations to solve by setting Λ

$$\frac{d\Lambda}{d\Phi_T} \equiv \frac{d}{dC_i^{\alpha*}} [\Lambda(C_1^\alpha, C_2^\alpha, \dots, C_N^\alpha, \epsilon_1, \epsilon_2, \dots, \epsilon_N)] = 0, \quad \forall i \in \mathbb{N}^*. \quad (20)$$

The Hartree-Fock equations (2)

Treating C_i^α and $C_i^{\alpha*}$ as independent, we arrive at the Hartree-Fock equations (one equation for each basis state $|\alpha\rangle$)

$$\sum_{\gamma} \langle \alpha | h | \gamma \rangle C_i^{\gamma} + \sum_{\gamma} \left[\overbrace{\sum_{j=1}^N \sum_{\beta \delta} C_j^{\beta*} \underbrace{\langle \alpha \beta | V | \gamma \delta \rangle}_{\text{Two-body interaction matrix element } V_{\alpha\beta\gamma\delta}}}^{\text{Effective potential } \langle \alpha | U | \gamma \rangle} C_j^{\delta} \right] C_i^{\gamma} = \epsilon_i C_i^{\alpha}, \quad (21)$$

which we can rewrite as $\sum_{\gamma} \mathcal{O}_{\alpha\gamma} C_i^{\gamma} = \epsilon_i C_i^{\alpha}, \quad \forall \alpha \in \mathcal{H}.$

\Rightarrow **System of non-linear equations** in the $C_i^{\alpha*}$, since $\mathcal{O}_{\alpha\gamma}$ depends itself on the unknowns.

\Rightarrow **To be solved by an iterative procedure.**

The Hartree-Fock (self-consistent) iterative procedure

- 1 Compute the effective Coulomb interaction potential $\langle \alpha | U^{(0)} | \gamma \rangle$ with an initial guess of the $C_i^{\alpha(0)}$.
- 2 Build the resulting Fock matrix \mathcal{O} .
- 3 Solve the linearised system given by the equations (Fock matrix diagonalization)

$$\sum_{\gamma} [\langle \alpha | h | \gamma \rangle + \langle \alpha | U | \gamma \rangle] C_i^{\gamma} = \epsilon_i C_i^{\alpha}.$$

at iteration (k) , store the output eigenenergies $\epsilon_i^{(k)}$ and the coefficients of the new eigenvectors $C_i^{\alpha(k)}$.

- 4 Substitute back the new coefficients to compute a new Coulomb interaction potential.
- 5 ...
- 6 Continue the process until self-consistency is reached.

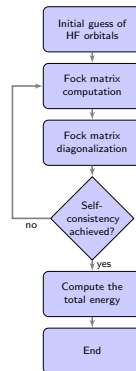


Figure 8: Flowchart of Hartree-Fock algorithm.

Many-body perturbation theory

Take the Hamiltonian $\hat{H} = \hat{H}_0 + \hat{H}'$, and treat \hat{H}' as a perturbation, such as the Coulomb interaction.

Suppose Φ_n eigenfunctions of \hat{H}_0 corresponding to the eigenvalues E_n : $\hat{H}_0 \Phi_n = E_n \Phi_n$. Consider the effect of the perturbation on a particular state Φ_0 .

We denote by Ψ_0 the state into which Φ_0 changes under the action of the perturbation, so that Ψ_0 is an eigenfunction of \hat{H} , corresponding to the eigenvalue E .

$$\hat{H}_0 \Phi_0 = E_0 \Phi_0. \quad (22)$$

$$\hat{H} \Psi_0 = E \Psi_0. \quad (23)$$

Therefore Φ_0 and Ψ_0 denote the ground states of the unperturbed and perturbed systems respectively.

Since \hat{H}_0 is Hermitian, one can show that:

$$E - E_0 = \frac{\langle \Phi_0 | \hat{H}' | \Psi_0 \rangle}{\langle \Phi_0 | \Psi_0 \rangle}. \quad (24)$$

which is an exact expression and independent of any particular perturbation method. Since Ψ_0 is unknown, using a *projection operator* \mathbf{R} for the state Φ_0 defined by the equation

$$\mathbf{R}\Psi = \Psi - \Phi_0 \langle \Phi_0 | \Psi \rangle, \quad (25)$$

The perturbed energy

The perturbed energy can be derived from the iterated Ψ_0 which gives

$$E - E_0 = \sum_{n=0}^{\infty} \langle \Phi_0 | \hat{H}' \left(\frac{\mathbf{R}}{E_0 - \hat{H}_0} (E_0 - E + \hat{H}') \right)^n | \Phi_0 \rangle. \quad (26)$$

We shall write

$$\Delta E = E - E_0 = \Delta E^{(1)} + \Delta E^{(2)} + \Delta E^{(3)} + \dots$$

where the m^{th} -order energy correction $\Delta E^{(m)}$ contains the m^{th} -order power of the perturbation \hat{H}' .

The many-body perturbation corrections

- The 1st-order correction is

$$\Delta E^{(1)} = \langle \Phi_0 | \hat{H}' | \Phi_0 \rangle. \quad (27)$$

- The 2nd-order correction is

$$\Delta E^{(2)} = \langle \Phi_0 | \hat{H}' \frac{\mathbf{R}}{E_0 - \hat{H}_0} (E_0 - E + \hat{H}') | \Phi_0 \rangle. \quad (28)$$

- The 3rd-order energy correction reads

$$\begin{aligned} \Delta E^{(3)} = & \sum_{n=0}^{\infty} \sum_{m=0}^{\infty} \frac{\langle \Phi_0 | \hat{H}' | \Phi_m \rangle \langle \Phi_m | \hat{H}' | \Phi_n \rangle \langle \Phi_n | \hat{H}' | \Phi_0 \rangle}{(E_0 - E_m)(E_0 - E_n)} \\ & - \langle \Phi_0 | \hat{H}' | \Phi_0 \rangle \sum_{n=0}^{\infty} \frac{\langle \Phi_0 | \hat{H}' | \Phi_n \rangle \langle \Phi_n | \hat{H}' | \Phi_0 \rangle}{(E_0 - E_n)^2}. \end{aligned} \quad (29)$$

The MBPT corrections expanded in a basis set

It is possible to rewrite the many-body energy corrections in particle and hole state formalism by using the expression of \hat{H}' as expressed in terms of annihilation (c_k) and creation (c_k^\dagger) operators

$$\hat{H}' = \frac{1}{2} \sum_{ijkl} \langle ij | v | kl \rangle c_i^\dagger c_j^\dagger c_l c_k,$$

The previous many-body perturbation corrections now read

$$\Delta E^{(1)} = \langle \Phi_0 | \hat{H}' | \Phi_0 \rangle = \frac{1}{2} \sum_{h_1 h_2} \langle h_1 h_2 | v | h_1 h_2 \rangle_{as}, \quad (30)$$

$$\Delta E^{(2)} = \sum_{n=0}^{\infty} \frac{\langle \Phi_0 | \hat{H}' | \Phi_n \rangle \langle \Phi_n | \hat{H}' | \Phi_0 \rangle}{E_0 - E_n} = \frac{1}{4} \sum_{h_1 h_2 p_1 p_2} \frac{|\langle h_1 h_2 | v | p_1 p_2 \rangle_{as}|^2}{\epsilon_{h_1} + \epsilon_{h_2} - \epsilon_{p_1} - \epsilon_{p_2}},$$

where h_i and p_i are respectively hole states and particles states, and ϵ_i are the single particle energies of the basis set.

The MBPT corrections expanded in a basis set

The 3rd-order many-body perturbation correction reads

$$\begin{aligned}\Delta E^{(3)} &= \sum_{n=0}^{\infty} \sum_{m=0}^{\infty} \frac{\langle \Phi_0 | \hat{H}' | \Phi_m \rangle \langle \Phi_m | \hat{H}' | \Phi_n \rangle \langle \Phi_n | \hat{H}' | \Phi_0 \rangle}{(E_0 - E_m)(E_0 - E_n)} \\ &\quad - \langle \Phi_0 | \hat{H}' | \Phi_0 \rangle \sum_{n=0}^{\infty} \frac{\langle \Phi_0 | \hat{H}' | \Phi_n \rangle \langle \Phi_n | \hat{H}' | \Phi_0 \rangle}{(E_0 - E_n)^2} \\ &= \Delta E_{4p-2h}^{(3)} + \Delta E_{2p-4h}^{(3)} + \Delta E_{3p-3h}^{(3)},\end{aligned}\tag{31}$$

where

- $\Delta E_{4p-2h}^{(3)}$ is the contribution to the third-order energy correction due to the 4-particle/2-hole excitations,
- $\Delta E_{2p-4h}^{(3)}$ is the contribution to the third-order energy correction due to the 2-particle/4-hole excitations,
- $\Delta E_{3p-3h}^{(3)}$ is the contribution to the third-order energy correction due to the 3-particle/3-hole excitations.

The MBPT corrections expanded in a basis set

The contributions to the third-order energy correction can be written as

$$\begin{aligned}\Delta E_{4p-2h}^{(3)} &= \frac{1}{8} \sum_{h_1 h_2 p_1 p_2} \left(\frac{\langle h_1 h_2 | v | p_1 p_2 \rangle_{as}}{\epsilon_{h_1} + \epsilon_{h_2} - \epsilon_{p_1} - \epsilon_{p_2}} \sum_{p_3 p_4} \frac{\langle p_1 p_2 | v | p_3 p_4 \rangle_{as} \langle p_3 p_4 | v | h_1 h_2 \rangle_{as}}{\epsilon_{h_1} + \epsilon_{h_2} - \epsilon_{p_3} - \epsilon_{p_4}} \right), \\ \Delta E_{2p-4h}^{(3)} &= \frac{1}{8} \sum_{h_1 h_2 p_1 p_2} \left(\frac{\langle h_1 h_2 | v | p_1 p_2 \rangle_{as}}{\epsilon_{h_1} + \epsilon_{h_2} - \epsilon_{p_1} - \epsilon_{p_2}} \sum_{h_3 h_4} \frac{\langle h_1 h_2 | v | h_3 h_4 \rangle_{as} \langle h_3 h_4 | v | h_1 h_2 \rangle_{as}}{\epsilon_{h_3} + \epsilon_{h_4} - \epsilon_{p_1} - \epsilon_{p_2}} \right), \\ \Delta E_{3p-3h}^{(3)} &= \sum_{h_1 h_2 p_1 p_2} \left(\frac{\langle h_1 h_2 | v | p_1 p_2 \rangle_{as}}{\epsilon_{h_1} + \epsilon_{h_2} - \epsilon_{p_1} - \epsilon_{p_2}} \left(\sum_{h_3} \sum_{p_3} \frac{\langle h_1 h_3 | v | p_1 p_3 \rangle_{as} \langle p_3 h_2 | v | h_3 h_2 \rangle_{as}}{\epsilon_{h_1} + \epsilon_{h_3} - \epsilon_{p_1} - \epsilon_{p_3}} \right) \right),\end{aligned}$$

where the p_i denote the particle states, h_i the hole states, and ϵ_i the single particle energies of the corresponding state.

Code implementation

Tools

- C++ language: for flexibility using classes and efficiency.
- BLITZ++ library: managing dense arrays.
- LPP / LAPACK library: (Fortran) routines for solving linear algebra problems.
- MESSAGE-PASSING INTERFACE: for parallel computing

Functionality

- Read parameters from a unique textual input file or command line.
- The `simulator` class performs the initialization and calls other objects.
- The `orbitalsQuantumNumbers` class: generates the harmonic oscillator states.
- The `CoulombMatrix` class generates the Coulomb interaction matrix outside Hartree-Fock.
- The `HartreeFock` class computes the HF energy and generates the interaction matrix in the HF basis.
- The `PerturbationTheory` class computes many-body perturbation corrections from 1st- to 3rd-order, either in the harmonic oscillator or in the HF basis set.

Implementation issues

Difficulties encountered if not making use of symmetries

- Huge Fock matrix to diagonalize (grows exponentially with R^b).
- Huge Coulomb interaction matrix to store
 $V_{\alpha\beta\gamma\delta} = \langle (n_1, m_{l1})(n_2, m_{l2}) | V | (n_3, m_{l3})(n_4, m_{l4}) \rangle$ is an 8-dimensional array.

Solutions implemented

By using the symmetries and properties of the Coulomb interaction:

- $V_{\alpha\beta\gamma\delta}$ does not act on spin: $m_{s1} = m_{s3}$ & $m_{s2} = m_{s4}$.
- $V_{\alpha\beta\gamma\delta}$ conserves the total spin and angular momentum: $m_{l1} + m_{l2} = m_{l3} + m_{l4}$.

By sorting the states of the basis by blocks of identical angular (m_l) and spin (m_s) quantum numbers:

- It allows to reduce the storage of the Coulomb interactions per blocks of couple of states by avoiding to store zeros's elements.
- The Fock matrix appears as block diagonal, allowing much smaller eigenvalue problems to solve.

Table of contents

- 1 Quantum Dots
- 2 Model, Methods and Implementation
- 3 Results and Discussions
 - Validation of the simulator
 - Limit of the closed-shell model as a function of λ
 - Convergence/Stability/Accuracy of HF
 - Comparison on HF/MBPT/FCI calculations

Validation of the simulator

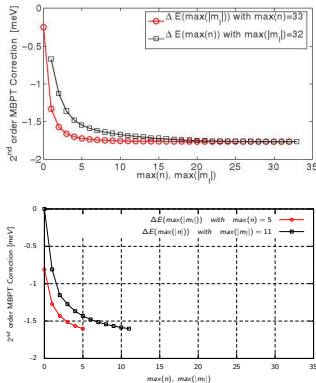


Figure 9: 2nd-order perturbation theory correction for the 2e⁻ QD. Comparison between results of Waltersson (top) [3] and our results (down).

Simple checks

- Reproduce the non-interacting ground state energies.
- Reproduce the two-body interaction matrix elements of OPENFCI almost with machine precision

Comparison of MBPT results with similar experiments

- Waltersson computed the open-shell 2nd-order MBPT correction.
- Our closed-shell 2nd-order MBPT correction shows close agreement.

Level crossing as a function of B without interactions (1/3)

Fock-Darwin orbitals

When neglecting the repulsions between the particles, the eigenenergies $\epsilon_{n m_l}$ as a function of the magnetic field B can be solved analytically for a parabolic confining potential $V(r) = 1/(2m^*\omega_0^2 r^2)$ leading to a spectrum known as the Fock-Darwin states

Rewriting the eigenenergies in units of $\hbar\omega_0$, $\epsilon_{n m_l}$ becomes dimensionless and we obtain

$$\epsilon_{n m_l} = (2n + |m_l| + 1) \sqrt{1 + \frac{(\omega_c/\omega_0)^2}{4}} - \frac{1}{2}(\omega_c/\omega_0) m_l \quad (32)$$

$$= (2n + |m_l| + 1) \sqrt{1 + \left(\frac{eB}{2m^*\omega_0}\right)^2} - \frac{eB}{2m^*\omega_0} m_l. \quad (33)$$

Level crossing as a function of B without interactions (2/3)

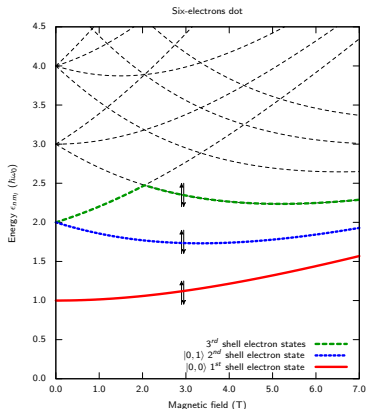


Figure 10: Spectrum of Fock-Darwin orbitals for 6 non-interacting particles (GaAs: $\hbar\omega_0 = 5\text{meV}$, $\epsilon_r = 12$).

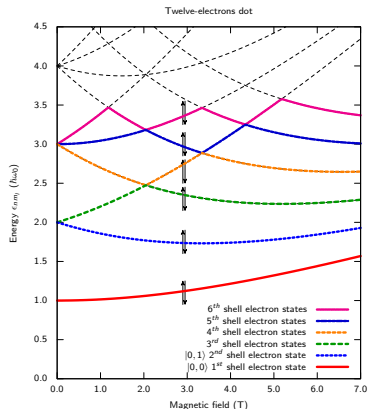
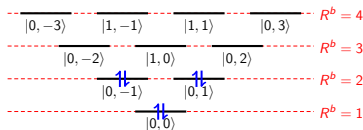


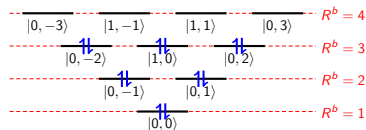
Figure 11: Spectrum of Fock-Darwin orbitals for 12 non-interacting particles (GaAs: $\hbar\omega_0 = 5\text{meV}$, $\epsilon_r = 12$).

Level crossing as a function of B without interactions (1/3)

6 non-interacting particles

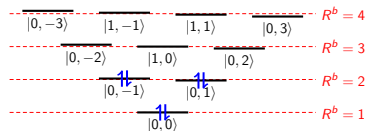


12 non-interacting particles

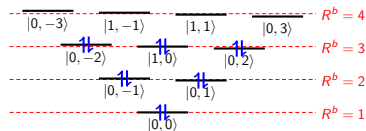


Level crossing as a function of B without interactions (1/3)

6 non-interacting particles

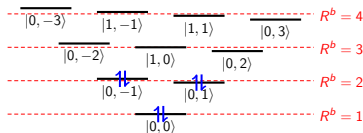


12 non-interacting particles

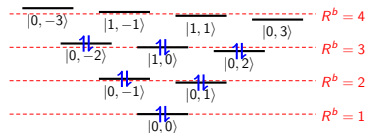


Level crossing as a function of B without interactions (1/3)

6 non-interacting particles

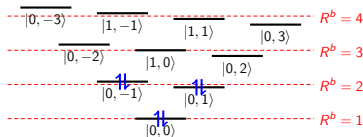


12 non-interacting particles

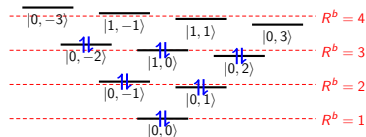


Level crossing as a function of B without interactions (1/3)

6 non-interacting particles

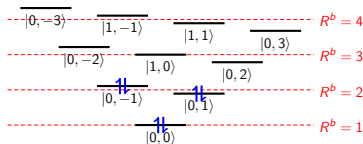


12 non-interacting particles

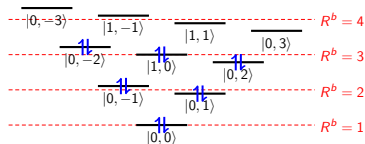


Level crossing as a function of B without interactions (1/3)

6 non-interacting particles

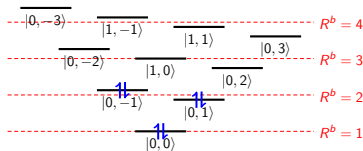


12 non-interacting particles

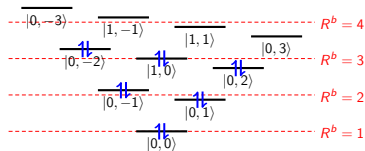


Level crossing as a function of B without interactions (1/3)

6 non-interacting particles

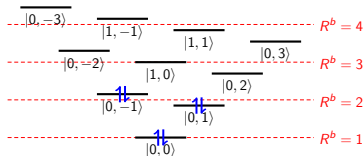


12 non-interacting particles

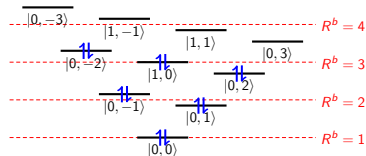


Level crossing as a function of B without interactions (1/3)

6 non-interacting particles

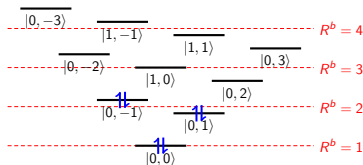


12 non-interacting particles

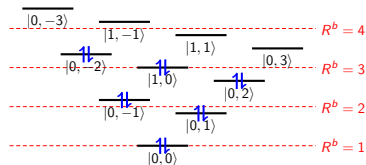


Level crossing as a function of B without interactions (1/3)

6 non-interacting particles

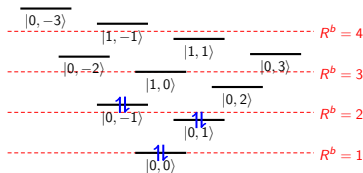


12 non-interacting particles

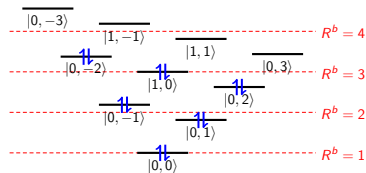


Level crossing as a function of B without interactions (1/3)

6 non-interacting particles

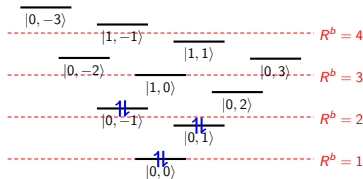


12 non-interacting particles

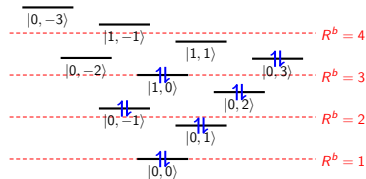


Level crossing as a function of B without interactions (1/3)

6 non-interacting particles

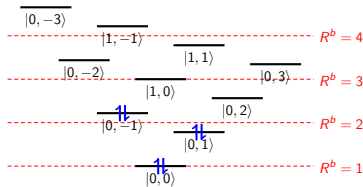


12 non-interacting particles

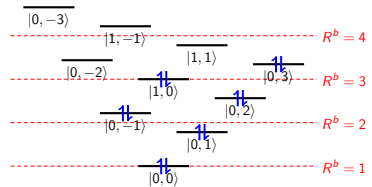


Level crossing as a function of B without interactions (1/3)

6 non-interacting particles

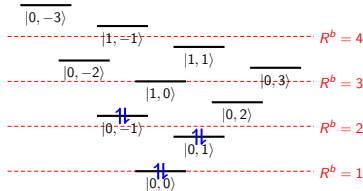


12 non-interacting particles

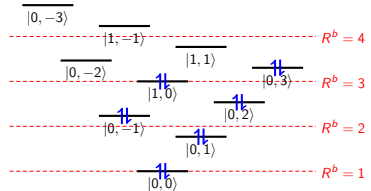


Level crossing as a function of B without interactions (1/3)

6 non-interacting particles

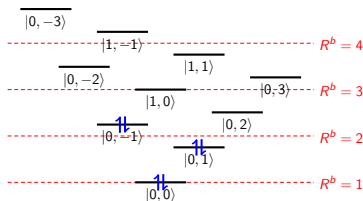


12 non-interacting particles

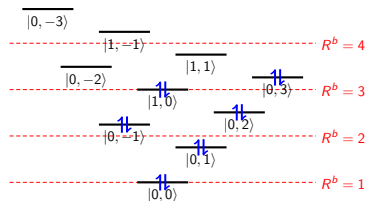


Level crossing as a function of B without interactions (1/3)

6 non-interacting particles

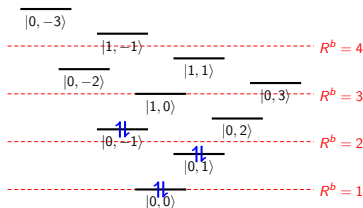


12 non-interacting particles

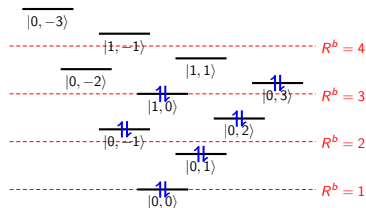


Level crossing as a function of B without interactions (1/3)

6 non-interacting particles

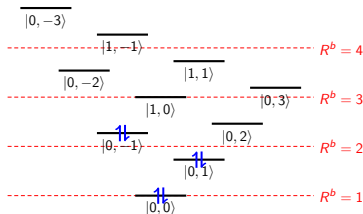


12 non-interacting particles

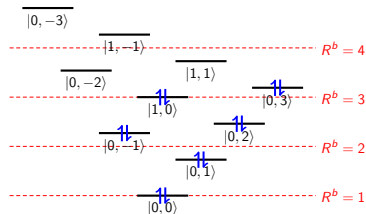


Level crossing as a function of B without interactions (1/3)

6 non-interacting particles

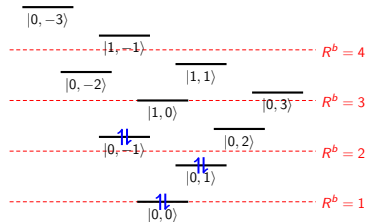


12 non-interacting particles

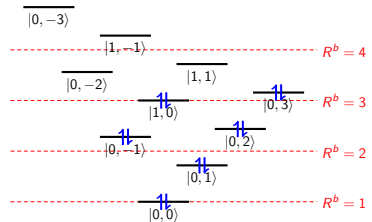


Level crossing as a function of B without interactions (1/3)

6 non-interacting particles

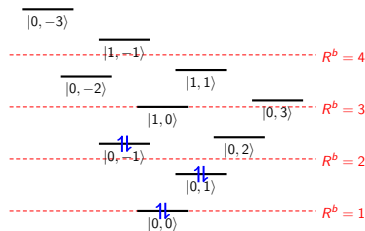


12 non-interacting particles

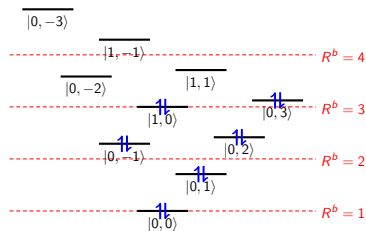


Level crossing as a function of B without interactions (1/3)

6 non-interacting particles

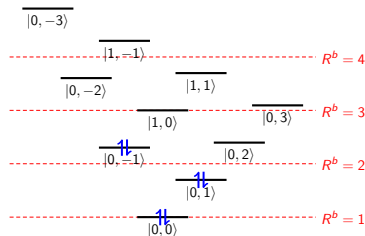


12 non-interacting particles

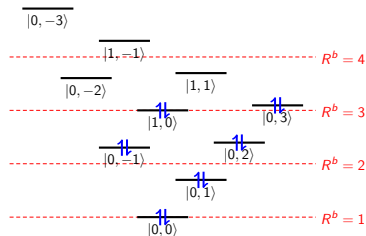


Level crossing as a function of B without interactions (1/3)

6 non-interacting particles

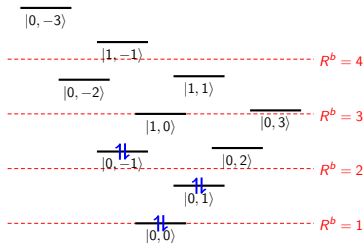


12 non-interacting particles

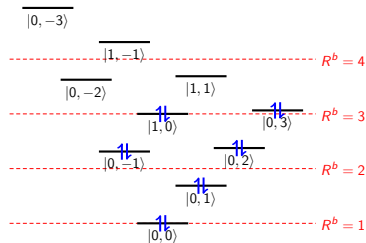


Level crossing as a function of B without interactions (1/3)

6 non-interacting particles

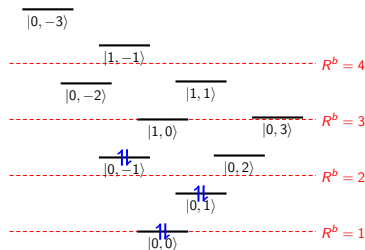


12 non-interacting particles

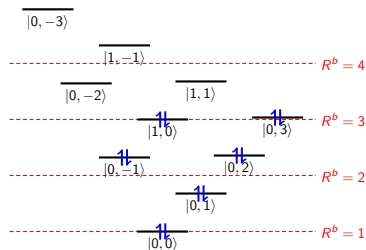


Level crossing as a function of B without interactions (1/3)

6 non-interacting particles

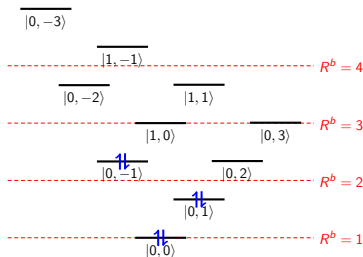


12 non-interacting particles

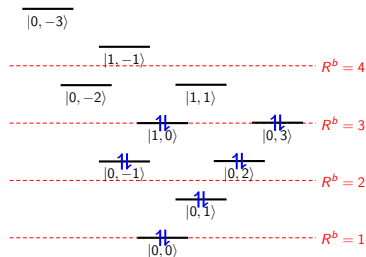


Level crossing as a function of B without interactions (1/3)

6 non-interacting particles

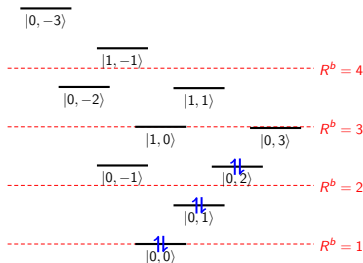


12 non-interacting particles

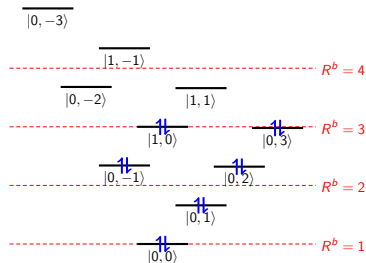


Level crossing as a function of B without interactions (1/3)

6 non-interacting particles

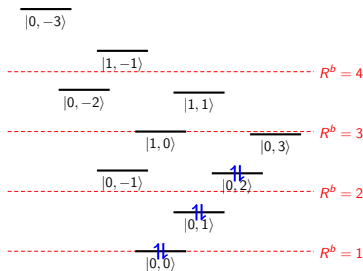


12 non-interacting particles

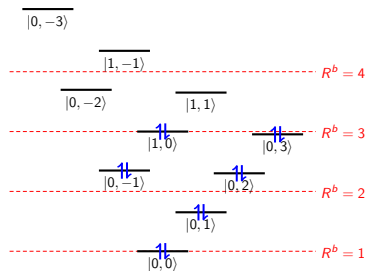


Level crossing as a function of B without interactions (1/3)

6 non-interacting particles

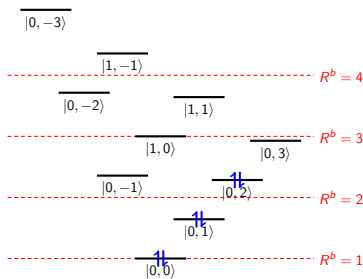


12 non-interacting particles

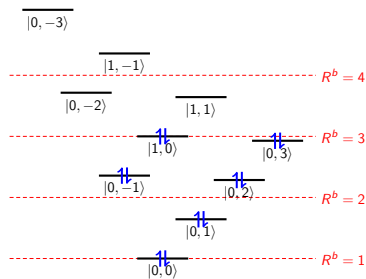


Level crossing as a function of B without interactions (1/3)

6 non-interacting particles

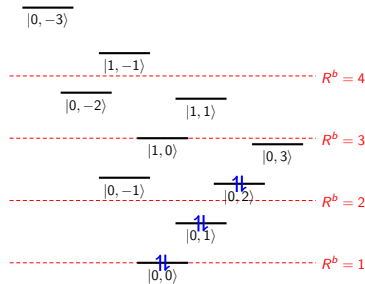


12 non-interacting particles

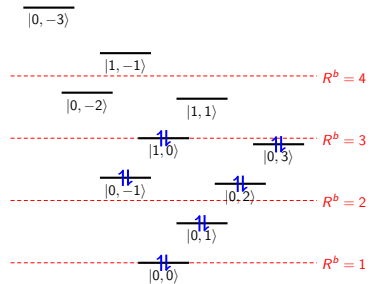


Level crossing as a function of B without interactions (1/3)

6 non-interacting particles

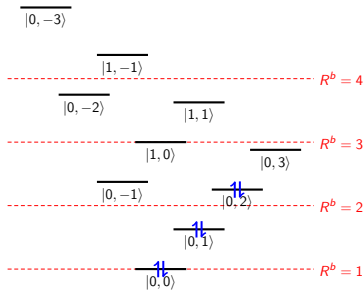


12 non-interacting particles

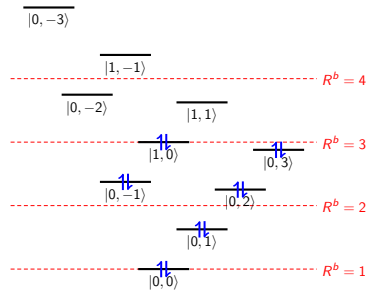


Level crossing as a function of B without interactions (1/3)

6 non-interacting particles

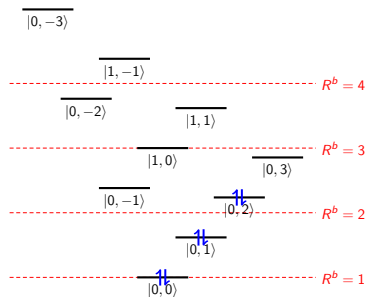


12 non-interacting particles

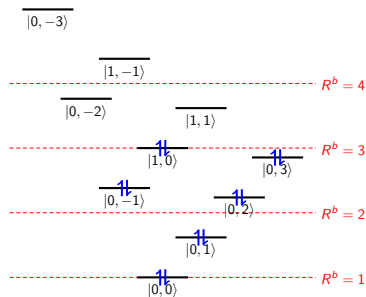


Level crossing as a function of B without interactions (1/3)

6 non-interacting particles

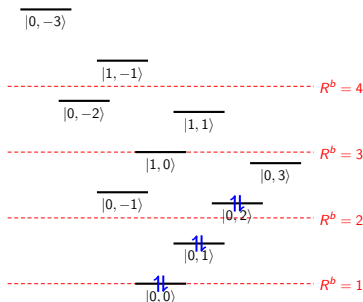


12 non-interacting particles

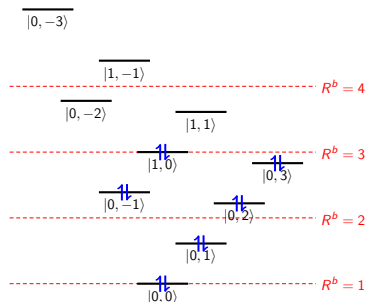


Level crossing as a function of B without interactions (1/3)

6 non-interacting particles

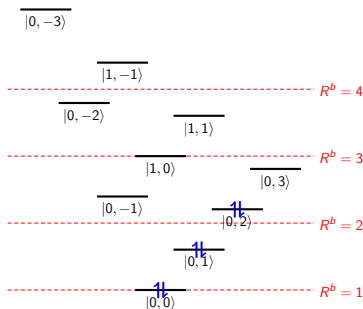


12 non-interacting particles

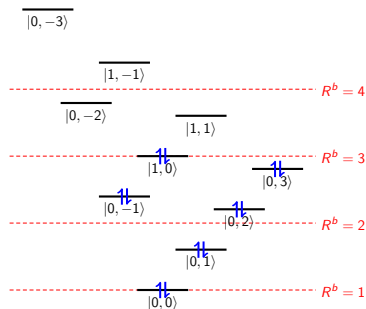


Level crossing as a function of B without interactions (1/3)

6 non-interacting particles

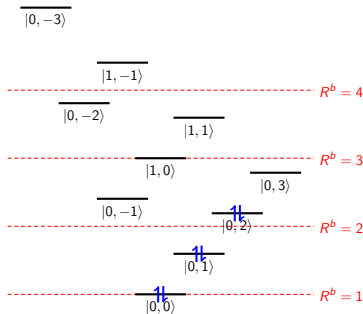


12 non-interacting particles

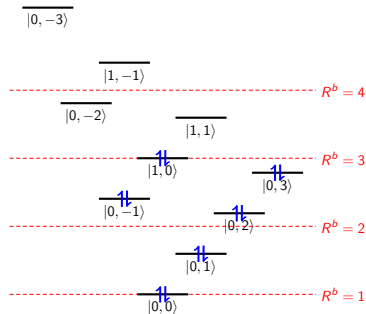


Level crossing as a function of B without interactions (1/3)

6 non-interacting particles

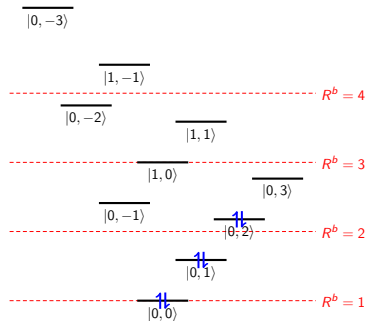


12 non-interacting particles

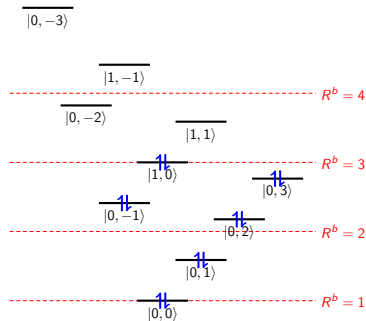


Level crossing as a function of B without interactions (1/3)

6 non-interacting particles



12 non-interacting particles



Level crossing as a function of λ with interactions (1/2)

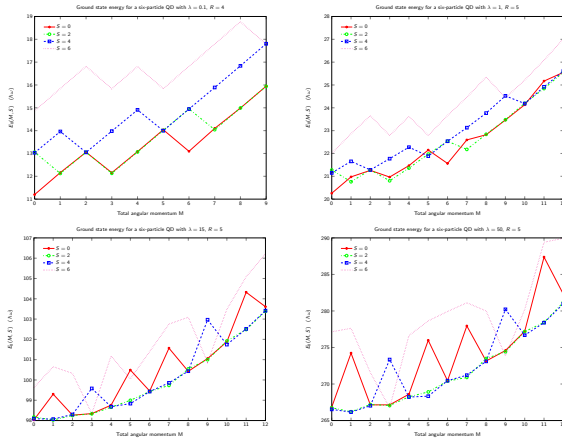


Figure 12: FCI ground state energies for a 6-electron QD with $\lambda = \{0.1, 1\}$ (top) and $\lambda = \{15, 50\}$ (bottom).

Level crossing as a function of λ with interactions (2/2)

Summary of FCI results using OPENFCI

λ	FCI ground state energy ($\hbar\omega$) R=5	(M,S)
0.1	11.197	(0,0)
0.5	15.561	(0,0)
1	20.257	(0,0)
2	28.032	(0,0)
5	46.482	(0,0)
10	73.067	(0,0)
11	78.143	(0,0)
12	83.168	(0,0)
13	88.152	(0,0)
15	98.027	(1,2)
20	122.325	(1,2)
50	266.157	(1,4)

- For a 6-particle QD, break of the model of a single Slater determinant from $\lambda \simeq 13$.
- A similar study performed on a 2-particle QD indicates a break of the closed-shell model from $\lambda \simeq 150$.

Exponential convergence of HF as a function of R^b (1/3)

Definition

The size of the basis set characterized by R^b ($R^b \in \mathbb{N}$ $R^b \geq R^f$)
It defines the maximum shell number in the model space for our Hartree-Fock computation. It implies the number of orbitals in which each single particle wavefunction will be expanded, with spin degeneracy the number of states N_S is

$$N_S = (R^b + 1)(R^b + 2) \quad (34)$$

The bigger the basis set, the more accurate the single particle wavefunction is expected. In mathematical notation, R^b and the size of the basis set \mathcal{B} are defined by

$$\mathcal{B} = \mathcal{B}(R^b) = \left\{ |\phi_{nm_l}(\mathbf{r})\rangle \quad : 2n + |m_l| \leq R^b \right\}, \quad (35)$$

where $|\phi_{nm_l}(\mathbf{r})\rangle$ are the single orbital in the Harmonic oscillator basis with quantum numbers n , m_l such that the single orbital energy reads: $\epsilon_{nm_l} = 2n + |m_l| + 1$ in two-dimensions.

Exponential convergence of HF as a function of R^b (2/3)

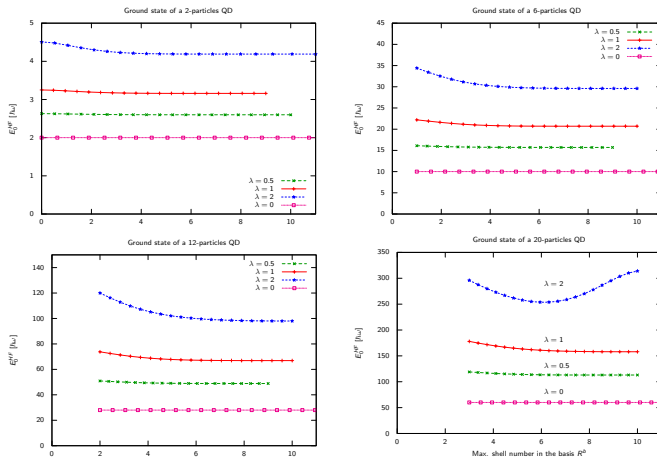


Figure 13: Hartree-Fock ground state (E_0^{HF} as a function of R^b for 2-,6-electron QD (top) and 12-,20-electron QD (bottom).

Exponential convergence of HF as a function of R^b (3/3)

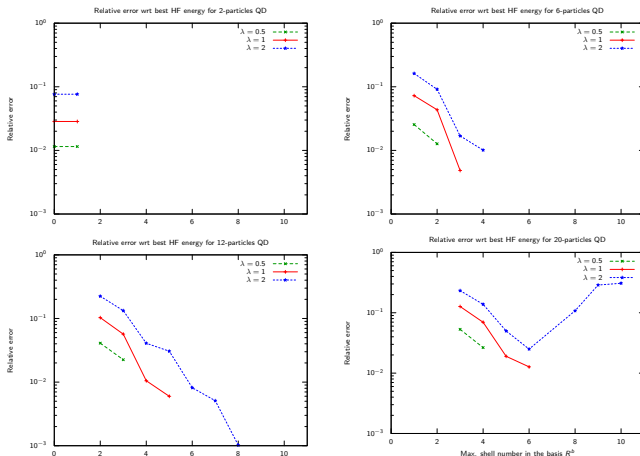


Figure 14: Hartree-Fock relative error $(E^{HF}(R^b) - E_{min}^{HF})/E_{min}^{HF}$ as a function of R^b for 2-,6-electron QD (top) and 12-,20-electron QD (bottom).

“Convergence history” as a function of λ (1/3)

Definition

The convergence history of a simulation shows how the convergence “improve” over iterations. We could plot

- the energy difference from one iteration to the next

$$\delta(\text{iter}) = |E^{HF}(\text{iter}) - E^{HF}(\text{iter} - 1)|.$$

- more intuitive on the form: $\delta(\text{iter}) \simeq 10^{-\beta \text{ iter}}$.

“Convergence history” as a function of λ (2/3)

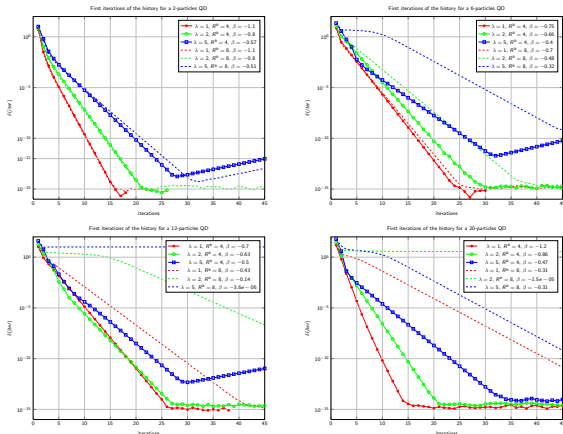


Figure 15: Convergence history of the Hartree-Fock iterative process for 2-,6-electron QD (top) and 12-,20-electron QD (bottom).

- slower convergence as λ increases.
- much less impact due to R^b or to the nb.of particles, except when leading to instability.

“Convergence history” as a function of λ (3/3)

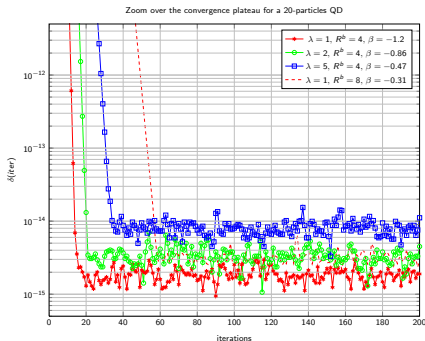


Figure 16: Zoom over the limit of convergence of the Hartree-Fock iterative process for a 20-particle QD.

- expected “plateau” when reaching machine precision.

However it seems that increasing the interaction strength:

- slows down the convergence process, as adding error at each iteration,
- induces a lower accuracy, as if it could “decrease the machine precision”,
⇒ Phenomena maybe due to round-off error, proportional to λ , and entering the eigenvalue solver in a non-trivial way.

Quadratic error growth of HF/MBPT wrt FCI ground state

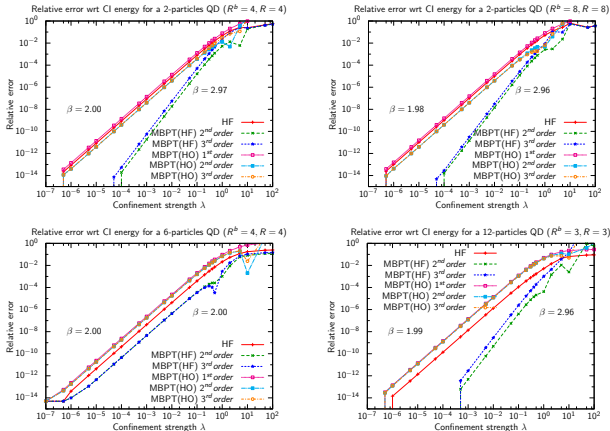


Figure 17: Comparison of HF/MBPT and HF corrected by MBPT up to 3rd-order wrt to the FCI ground state taken as reference for 2-electron QD (top) and 6-, 12-electron QD (bottom).

Respective accuracy of HF and MBPT (1/2)

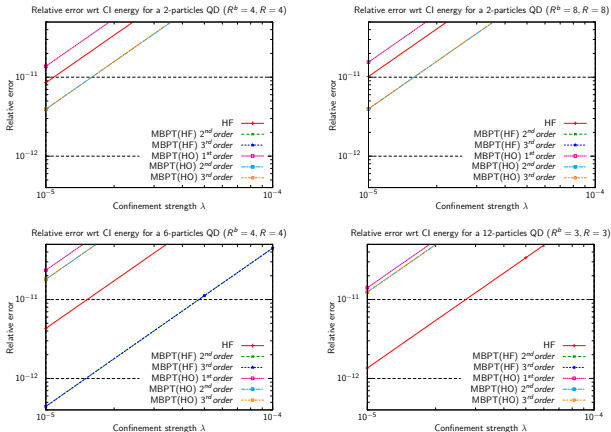


Figure 18: Zoom on the quadratic growth of the error when λ is relatively small ($\lambda < 0.05$), showing different accuracies with respect to the method, the number of particles and the size of the basis. for 2-electron QD (top) and 6-,12-electron QD (bottom).

# e ⁻	R^{FCI}	R^{HF}	Relative error shift between each method for $\lambda = 10^{-3}$	
2	4	4	MBPT(HF)-2 nd order	$\rightarrow \epsilon_{min}$
			MBPT(HF)-3 rd order	$\rightarrow 3 \epsilon_{min}$
			MBPT(H0)-2 nd order and MBPT(H0)-3 rd order	$\rightarrow 2.1 \times 10^3 \epsilon_{min}$
			HF	$\rightarrow 4.6 \times 10^3 \epsilon_{min}$
	8	8	MBPT(HO)-1 st order	$\rightarrow 7.5 \times 10^3 \epsilon_{min}$
			MBPT(HF)-2 nd order and MBPT(HF)-3 rd order	$\rightarrow \epsilon_{min}$
			MBPT(H0)-2 nd order and MBPT(H0)-3 rd order	$\rightarrow 2.7 \times 10^3 \epsilon_{min}$
			HF	$\rightarrow 7 \times 10^3 \epsilon_{min}$
6	4	4	MBPT(HO)-1 st order	$\rightarrow 10.7 \times 10^3 \epsilon_{min}$
			MBPT(HF)-2 nd order and MBPT(HF)-3 rd order	$\rightarrow \epsilon_{min}$
			HF	$\rightarrow 9.65 \epsilon_{min}$
			MBPT(H0)-2 nd order and MBPT(H0)-3 rd order	$\rightarrow 40.3 \epsilon_{min}$
	8	8	MBPT(HO)-1 st order	$\rightarrow 52.55 \epsilon_{min}$
			MBPT(HF)-2 nd order and MBPT(HF)-3 rd order	$\rightarrow \epsilon_{min}$
			HF	$\rightarrow 1.31 \epsilon_{min}$
			MBPT(H0)-2 nd order and MBPT(H0)-3 rd order	$\rightarrow 5.47 \epsilon_{min}$
12	3	3	MBPT(HO)-1 st order	$\rightarrow 8 \epsilon_{min}$
			MBPT(HF)-2 nd order	$\rightarrow \epsilon_{min}$
			MBPT(HF)-3 rd order	$\rightarrow 5.98 \epsilon_{min}$
			HF	$\rightarrow 5.6 \times 10^3 \epsilon_{min}$
			MBPT(H0)-2 nd order and MBPT(H0)-3 rd order	$\rightarrow 51.3 \times 10^3 \epsilon_{min}$
			MBPT(HO)-1 st order	$\rightarrow 58.4 \times 10^3 \epsilon_{min}$

Table 1: Classification of the methods with respect to their relative accuracy in the range of λ that exhibits a quadratic error growth.

Break of the methods

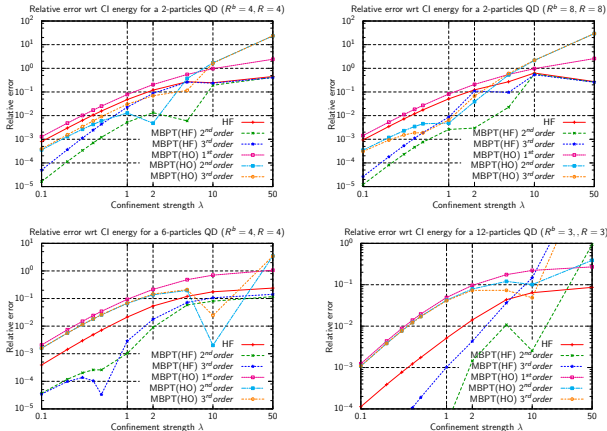


Figure 19: The plots display a zoom for λ approaching the limit of the closed-shell model for 2-electron QD (top) and 6-,12-electron QD (bottom).







Summary of the results





- Exponential convergence of HF as a function of R^b .
- Increasing λ slows down the convergence of HF, and decreases its accuracy.
- Compared to FCI, HF and MBPT have a quadratic error growth wrt λ .
- Unstability of the 2nd- 3rd-order MBPT corrections before 1st-order MBPT and HF.

Break of the method before the closed-shell model

# particles	Break of the method	Break of the model
2	$\lambda \simeq 5$	$\lambda \simeq 150$
6	$\lambda \simeq 2$	$\lambda \simeq 14$
12	$\lambda \simeq 1$	$\lambda \simeq ???$

Thank you for your attention ;)

-  L. P. Kouwenhoven. *Electron transport in quantum dots*, Proceedings of the Advanced Study Institute, 1997.
-  X. Gao, Y. Cui, R. M. Levenson, L. W. Chung, and S. Nie. In vivo cancer targeting and imaging with semiconductor quantum dots. *Nat Biotech*, 22:969–976, 2004.
-  L. P. Kouwenhoven, D. G. Austing, and S. Tarucha. Few-electron quantum dots. *Reports on Progress in Physics*, 64:701–736, 2001.
-  S. Kvaal. Open source fci code for quantum dots and effective interactions. *arXiv.org*, 2008.
-  S. Kvaal. *Analysis of many-body methods for quantum dots*. PhD thesis, University of Oslo, 2009.
-  M. Moshinsky and Y. F. Smirnov. *The Harmonic Oscillator in Modern Physics: From Atoms to Quarks*. Taylor & Francis, 1996.

-  D. Pfannkuche, V. Gudmundsson, and P. A. Maksym. Comparison of a hartree, a hartree-fock, and an exact treatment of quantum-dot helium. *Phys. Rev. B*, 47:2244–2250, 1993.
-  S. Raimes. *Many-electron Theory*. North-Holland Publishing, 1972.
-  E. Waltersson and E. Lindroth. Many-body perturbation theory calculations on circular quantum dots. *Phys. Rev. B*, 76:045314, 2007.
-  J. O. Winter. *Development and optimization of quantum dot-neuron interfaces*. PhD thesis, The University of Texas at Austin, 2004.